



Published in final edited form as:

Proc SPIE Int Soc Opt Eng. 2017 February 11; 10137: . doi:10.1117/12.2255802.

A radiative transfer equation-based image-reconstruction method incorporating boundary conditions for diffuse optical imaging

Abhinav K. Jha^a, Yansong Zhu^b, Dean F. Wong^a, and Arman Rahmim^{a,b}

^aDepartment of Radiology, Johns Hopkins University, Baltimore, MD, USA

^bDepartment of Electrical and Computer Engineering, Baltimore, MD, USA

Abstract

Developing reconstruction methods for diffuse optical imaging requires accurate modeling of photon propagation, including boundary conditions arising due to refractive index mismatch as photons propagate from the tissue to air. For this purpose, we developed an analytical Neumann-series radiative transport equation (RTE)-based approach. Each Neumann series term models different scattering, absorption, and boundary-reflection events. The reflection is modeled using the Fresnel equation. We use this approach to design a gradient-descent-based analytical reconstruction algorithm for a three-dimensional (3D) setup of a diffuse optical imaging (DOI) system. The algorithm was implemented for a three-dimensional DOI system consisting of a laser source, cuboidal scattering medium (refractive index > 1), and a pixelated detector at one cuboid face. In simulation experiments, the refractive index of the scattering medium was varied to test the robustness of the reconstruction algorithm over a wide range of refractive index mismatches. The experiments were repeated over multiple noise realizations. Results showed that by using the proposed algorithm, the photon propagation was modeled more accurately. These results demonstrated the importance of modeling boundary conditions in the photon-propagation model.

Keywords

Modeling photon propagation; Boundary conditions; Image reconstruction; Diffuse optical imaging

1. INTRODUCTION

In optical imaging modalities such as diffuse optical imaging (DOI),¹⁻³ fluorescence imaging⁴ and fluorescence tomography,^{5,6} using the boundary measurements to estimate the optical coefficients of the imaged tissue typically requires a model for photon propagation. The radiative transport equation (RTE) is a well-known method for modeling this light propagation.⁷ However, executing the RTE is computationally intensive. To overcome this issue, an approximation to this equation, known as the diffusion approximation,⁸⁻¹¹ is commonly used. This approximation assumes that light propagates diffusely in tissues.

However, this assumption is inaccurate near tissue surface, in anisotropic tissues, and in regions of high absorption or low scatter.^{1,3,12,13} Consequently, the diffusion approximation cannot accurately describe light propagation in highly absorbing regions such as haematomas, void-like spaces such as ventricles and the subarachnoid-space,^{13–17} and for small tissue geometries, such as whole-body imaging of small animals.¹² For more accurate modeling, higher-order approximations to the RTE, such as the discrete ordinates method (S_N)^{13,16,18–20} and spherical harmonic equations (P_N)^{21,22} have been developed. These methods require solving systems of coupled equations. However, the number of equations to solve can be very high, so that these methods are still computationally expensive.

While the above methods focus on solving the differential form of the RTE, more recently, there has been research on solving the RTE in the integral form for optical imaging.^{23,24} The advantage of the integral-based methods in comparison to the differential methods is that they do not require solving many coupled equations. Also, the emission source in DOI are typically collimated, and it is easier to model such sources using the integral-based methods. A Neumann-series-based RTE to model photon propagation has been developed for both homogeneous²³ and heterogeneous scattering media.²⁴ We have shown that the Neumann-series RTE provides accurate modeling of photons in scenarios where the diffusion approximation methods fail. However, an issue with the existing Neumann-series method is that it does not account for the reflection of photons when there is a refractive-index mismatch. This refractive index mismatch could be especially pronounced as light propagates from the tissue to the air. Due to the reflection occurring at these interfaces, photons are reflected back into the medium. It has been observed previously that not modeling boundary conditions in photon transport can lead erroneous measurements of scattered light.²⁵ Further 50% or more errors in estimation of the optical coefficients of the underlying tissue.²⁶

The current integral version of the RTE is not able to accurately account for boundary effects. To overcome this issue, we had initially proposed an improved version of the Neumann-series approach.^{27,28} We continue to improve the approach. In this manuscript, the improved Neumann-series RTE that accounts for the boundary conditions arising due to refractive index mismatch for a DOI setup is first described. We then use this Neumann-series approach to design a method to reconstruct the absorption and scattering coefficients of a scattering medium in a DOI setup. Validation of the improved Neumann-series RTE using digital-phantom experiments is also presented.

2. METHODS

2.1 Neumann-series RTE

The fundamental radiometric quantity that we will describe the RTE is the photon distribution function, a quantity that is analogous to the radiance and quantifies the density of photons at a particular location and in a particular direction. Denote the photon distribution function at location \mathbf{r} in direction $\hat{\mathbf{s}}$ and frequency ν by $w(\mathbf{r}, \hat{\mathbf{s}}, \nu)$. Let the absorption and scattering coefficients at location \mathbf{r} be denoted by $\mu_a(\mathbf{r})$ and $\mu_{sc}(\mathbf{r})$ respectively and let c_m denote the speed of light in the medium. Let $\Xi(\mathbf{r}, \hat{\mathbf{s}}, \nu)$ denote a

mono-energetic source of emission of radiation, and let $f(\hat{s}, \hat{s}', \mathbf{r})$ denote the scattering phase function. The RTE can be written in the frequency domain as²³

$$\hat{s} \cdot \nabla w(\mathbf{r}, \hat{s}, v) + \left[\mu_a + \mu_{sc} + \frac{jv}{c_m} \right] w(\mathbf{r}, \hat{s}, v) = \frac{1}{c_m} \left[\Xi(\mathbf{r}, \hat{s}, v) + \mu_{sc}(\mathbf{r}) \int_{4\pi} d^2 \hat{s}' f(\hat{s}, \hat{s}'; \mathbf{r}) w(\mathbf{r}, \hat{s}', v) \right], \quad (1)$$

where j is the imaginary unit. This equation can also be represented in an integral form in terms of a Neumann series. Let \mathcal{X} and \mathcal{H} denote the attenuation and scattering operators, respectively. A schematic illustrating the definition of these operators is shown in Fig. 1 The mathematical expression of these operators for NIR imaging have been derived previously.^{23,24} In steady state, the integral form of the RTE is given by

$$w(\mathbf{r}, \hat{s}) = \mathcal{X} \Xi + \mathcal{X} \mathcal{H} w \quad (2)$$

This equation can be alternatively written in a Neumann-series form as follows:

$$w(\mathbf{r}, \hat{s}) = \mathcal{X} \Xi + \mathcal{X} \mathcal{H} \mathcal{X} \Xi + \mathcal{X} \mathcal{H} \mathcal{X} \mathcal{H} \mathcal{X} \Xi + \dots \quad (3)$$

An intuitive way of interpreting this equation is that successive terms in this series represent successive scattering events; in fact photons that have scattered n times contribute to the term $\mathcal{X} (\mathcal{H} \mathcal{X})^n \Xi$ in this series. This is as shown in Fig. 2.

To incorporate the boundary conditions into this Neumann series, we begin with a first principles treatment of light propagation in tissue. Similar to Schweigher *et al.*,²⁹ we define the boundary of the phantom to be an infinitesimally small thin layer just outside the phantom such that in this layer, only the reflection event occurs. This thin boundary layer is illustrated in Fig. 3. As a consequence of the boundary conditions, there will be reflection at the boundary. Therefore, the boundary acts as a source of photon emission given by the expression $\mathcal{R}w$ as:

$$[\mathcal{R}w](\mathbf{r}, \hat{s}') = \int_{\hat{n} \cdot \hat{s} > 0} R \delta[\hat{s}' - \hat{s} + 2(\hat{n} \cdot \hat{s}) \hat{n}] w(\mathbf{r}, \hat{s}) d\Omega_{\hat{s}}, \quad (4)$$

where \hat{s} and \hat{s}' are the vectors of incident and reflection direction, \hat{n} is the vector of normal direction of the boundary surface, and R is reflectivity given by Fresnel's law as:

$$R = \frac{1}{2} \left(\frac{n_i \cos \theta_i - n_t \cos \theta_t}{n_i \cos \theta_i + n_t \cos \theta_t} \right)^2 + \frac{1}{2} \left(\frac{n_t \cos \theta_i - n_i \cos \theta_t}{n_t \cos \theta_i + n_i \cos \theta_t} \right)^2, \quad (5)$$

where n_i, n_t denote refractive index of incident medium and transmitted medium, respectively, and θ_i, θ_t denote incident and transmitted angle, respectively. An alternative way to think about the boundary reflection is to consider it analogous to a scattering operation, except that the scattering phase function is given by the laws of reflection. Either of these two interpretations, when modeled in Eq. (2) leads to the following form for the RTE:

$$w = \mathcal{X}\Xi + \mathcal{X}\mathcal{R}w + \mathcal{X}\mathcal{H}w. \quad (6)$$

A formal solution to this equation is given by the Neumann series:

$$w = [\mathcal{I} + \mathcal{X}\mathcal{R} + \mathcal{X}\mathcal{H} + \mathcal{X}\mathcal{R}\mathcal{X}\mathcal{R} + \mathcal{X}\mathcal{H}\mathcal{X}\mathcal{H} + \mathcal{X}\mathcal{R}\mathcal{X}\mathcal{H} + \mathcal{X}\mathcal{H}\mathcal{X}\mathcal{R} + \dots]\mathcal{X}\Xi, \quad (7)$$

where \mathcal{I} is the identity operator. Each of these terms involving the reflection operator in the RTE has a physical interpretation. The term $\mathcal{X}\mathcal{R}\mathcal{X}\Xi$ represent the photons that are reflected at the boundary and subsequently transmitted back into the phantom. The radiance that is reflected back into the phantom, and subsequently gets scattered is given by the term $\mathcal{X}\mathcal{H}\mathcal{X}\mathcal{R}\mathcal{X}\Xi$. The term, $\mathcal{X}\mathcal{R}\mathcal{X}\mathcal{H}\mathcal{X}\Xi$ is the radiance that is scattered in the medium and after subsequently, is reflected back into the medium. We could add more terms if the refractive index mismatch between the tissue and external interface is very high.

2.2 Designing the Neumann-series-based reconstruction algorithm accounting for boundary conditions

Consider the scattering media to be discretized into N voxels, where the scattering/absorption coefficient of the n^{th} voxel is denoted by μ_n , and let the N -dimensional vector of these coefficients be denoted by $\boldsymbol{\mu}$. Denote the image acquired by the pixelated detector in the DOI setup by the M -dimensional vector \mathbf{g} . Our objective is to estimate $\boldsymbol{\mu}$ given \mathbf{g} . For this purpose, we derive a gradient-based approach. To begin with, let the mean noiseless image as a function of the scattering and absorption coefficient be given by $\bar{\mathbf{g}}(\boldsymbol{\mu})$. Then, the objective is to estimate that value of $\boldsymbol{\mu}$ that minimizes the L2 norm of the error between the measured data \mathbf{g} and the $\bar{\mathbf{g}}(\boldsymbol{\mu})$. Mathematically

$$\hat{\boldsymbol{\mu}} = \underset{\boldsymbol{\mu}}{\operatorname{argmin}} \|\mathbf{g} - \bar{\mathbf{g}}(\boldsymbol{\mu})\|_2, \quad (8)$$

where $\|\mathbf{x}\|_2$ denotes the L2 norm of the vector \mathbf{x} . The above can be solved by obtaining the gradient (also referred to as the Jacobian) of $\bar{\mathbf{g}}(\boldsymbol{\mu})$ with respect to μ_a and μ_s . Let $h_m(\mathbf{r}, \boldsymbol{\Omega})$ denote the detector response function of the m^{th} detector pixel. Then, the m^{th} component of $\bar{\mathbf{g}}(\boldsymbol{\mu})$, denoted by \bar{g}_m , is given by

$$\bar{g}_m = (h_m, w), \quad (9)$$

where (\cdot) denotes the inner product of two vectors. Taking the derivative on both sides yields

$$\frac{\partial \bar{g}_m}{\partial \mu} = \left(h_m, \frac{\partial w}{\partial \mu} \right) \quad (10)$$

It can be shown, by taking an approach similar to that proposed in Jha *et al.*,³⁰ that the derivative of the gradient of w with respect to μ is given by:

$$\frac{\partial w}{\partial \mu} = \mathcal{X} \mathcal{S} + \mathcal{X} \mathcal{R} \frac{\partial w}{\partial \mu} + \mathcal{X} \mathcal{K} \frac{\partial w}{\partial \mu}, \quad (11)$$

where

$$\mathcal{S} = -c_m \phi_n w + \varepsilon \phi_n \mathcal{K}_1 w \quad (12)$$

where ϕ_n is a spatial basis function for the n^{th} voxel, $\varepsilon = 1$ for $\mu = \mu_a$ and $\varepsilon = 0$ for $\mu = \mu_s$, and the effect of operator \mathcal{K}_1 is:

$$[\mathcal{K}_1 w](\mathbf{r}, \hat{\mathbf{s}}) = c_m \int d\Omega' f(\hat{\mathbf{s}}, \hat{\mathbf{s}}') w(\mathbf{r}, \hat{\mathbf{s}}'). \quad (13)$$

By comparing Eq. 11 to Eq. 1, we note that the expression for the gradient is the same as the original RTE, but with a different source term.

2.3 Implementation

The Neumann-series formalism was implemented for a 3-dimensional scattering medium with an experimental setup as shown in Fig. 4. The scattering medium was a cube, with each side of length 2 cm. Further, the scattering and absorption coefficients in the medium were 1 cm^{-1} and 0.01 cm^{-1} . For computational reasons, only three terms involving the reflection operator were implemented. Thus, the following form of the RTE was implemented:

$$w = \mathcal{X} E + \mathcal{X} \mathcal{K} \mathcal{X} \Xi + \mathcal{X} \mathcal{R} \mathcal{X} \Xi + \mathcal{X} \mathcal{R} \mathcal{X} \mathcal{K} \mathcal{X} \Xi + \mathcal{X} \mathcal{K} \mathcal{X} \mathcal{R} \mathcal{X} \Xi + \mathcal{X} \mathcal{K} \mathcal{X} \mathcal{K} \mathcal{X} \Xi + \dots \\ = \mathcal{X} \mathcal{R} \mathcal{X} \Xi + \mathcal{X} \mathcal{R} \mathcal{X} \mathcal{K} \mathcal{X} \Xi + \mathcal{X} \mathcal{K} \mathcal{X} \mathcal{R} \mathcal{X} \Xi + \text{Neumann series without boundary conditions.}$$

(14)

The process to implement the Neumann-series without boundary conditions was similar to as described in detail in Jha *et al.*²³ The output image was measured on a pixellated detector, as shown in the figure. The refractive index outside the medium was kept as 1. In this setup, the refractive index of the media was set as 1.05 and 1.1 to generate two different refractive index mismatches.

The output images generated using the proposed Neumann-series approach were compared to those obtained with the tmcimg Monte-Carlo technique. The output of the Monte-Carlo technique was considered as the gold standard.

3. RESULTS

A representative output image obtained with the proposed method is shown in Fig. 5. We observe that the image has a maxima at the center, arising primarily due to the unscattered component of the laser beam. This maxima gradually fades away as we approach the sides of the detector face. The result is on expected lines.

In Figs. 6a–d, the linear profile of the output image (as shown by the dotted line in Fig. 5), is plotted and overlaid on the corresponding MC output. We observe that in all cases, there is a good match between the outputs obtained with the MC and Neumann-series RTE approaches.

4. CONCLUSIONS

An analytical formalism based on integral form of radiative transport equation (RTE) was proposed to model photon propagation in tissue. The method accounts for reflective boundary conditions arising due to changes in refractive index when photons move from the tissue to air. The method was used to develop an algorithm to reconstruct the absorption and scattering coefficients of a scattering medium in a diffuse optical imaging (DOI) setup. The formalism was validated using a 3-D DOI setup. Results demonstrated that the proposed formalism provided more accurate photon propagation model in comparison to when the boundary conditions were not modeled. The results demonstrate the importance of modeling boundary conditions in the photon-propagation model.

In another effort as part of this BRAIN Initiative project, we are developing reconstruction methods for fluorescence molecular tomography. These methods exploit the sparsity in the fluorescence distribution, and additionally model the Poisson noise in the acquired image data. Results show that the proposed methods provide improved results in comparison to existing techniques for reconstruction.⁶

Acknowledgments

This work was financially supported by the NIH BRAIN Initiative Award R24 MH106083. The authors thank Simon Arridge, PhD, for helpful discussions.

References

1. Gibson AP, Hebden JC, Arridge SR. Recent advances in diffuse optical imaging. *Phys Med Biol.* Feb.2005 50:1–43. [PubMed: 15715418]
2. Boas DA, Brooks DH, Miller EL, DiMarzio CA, Kilmer M, Gaudette RJ, Zhang Q. Imaging the body with diffuse optical tomography. *IEEE Signal Process Mag.* 2001; 18:57–75.
3. Gibson A, Deghani H. Diffuse optical imaging. *Phil Tran A Math Phys Eng Sci.* Aug.2009 367:3055–3072.
4. Tanbakuchi AA, Rouse AR, Gmitro AF. Monte Carlo characterization of parallelized fluorescence confocal systems imaging in turbid media. *J Biomed Opt.* 2009; 14:044024. [PubMed: 19725735]

5. Chen J, Venugopal V, Intes X. Monte Carlo based method for fluorescence tomographic imaging with lifetime multiplexing using time gates. *Biomed Opt Express*. Apr.2011 2:871–886. [PubMed: 21483610]
6. Zhu Y, Jha AK, Dreyer JK, Le HND, Kang JU, Roland PE, Wong DF, Rahmim A. A three-step reconstruction method for fluorescence molecular tomography based on compressive sensing. 2017
7. Barrett, H., II, Myers, KJ. *Foundations of Image Science*. first. Wiley; 2004.
8. Arridge SR, Schweiger M, Hiraoka M, Delpy DT. A finite element approach for modeling photon transport in tissue. *Med Phys*. 1993; 20:299–309. [PubMed: 8497214]
9. Dehghani H, Brooksby B, Vishwanath K, Pogue BW, Paulsen KD. The effects of internal refractive index variation in near-infrared optical tomography: a finite element modelling approach. *Phys Med Biol*. Aug.2003 48:2713–2727. [PubMed: 12974584]
10. Schweiger M, Arridge SR. The finite-element method for the propagation of light in scattering media: frequency domain case. *Med Phys*. Jun.1997 24:895–902. [PubMed: 9198025]
11. Gao F, Niu H, Zhao H, Zhang H. The forward and inverse models in time-resolved optical tomography imaging and their finite-element method solutions. *Image Vis Comput*. 1998; 16:703–712.
12. Klose A, Larsen E. Light transport in biological tissue based on the simplified spherical harmonics equations. *J Comput Phys*. 2006; 220(1):441–470.
13. Hielscher AH, Alcouffe RE, Barbour RL. Comparison of finite-difference transport and diffusion calculations for photon migration in homogeneous and heterogeneous tissues. *Phys Med Biol*. May.1998 43:1285–1302. [PubMed: 9623656]
14. Aydin ED, de Oliveira CR, Goddard AJ. A comparison between transport and diffusion calculations using a finite element-spherical harmonics radiation transport method. *Med Phys*. Sep. 2002 29:2013–2023. [PubMed: 12349922]
15. Aydin ED. Three-dimensional photon migration through voidlike regions and channels. *Appl Opt*. Dec.2007 46:8272–8277. [PubMed: 18059668]
16. Hielscher, AH., Alcouffe, RE. *Adv Opt Imaging Photon Migration*. ATuC2, Optical Society of America; 1998. Discrete-ordinate transport simulations of light propagation in highly forward scattering heterogenous media.
17. Chu M, Vishwanath K, Klose AD, Dehghani H. Light transport in biological tissue using threedimensional frequency-domain simplified spherical harmonics equations. *Phys Med Biol*. Apr.2009 54:2493–2509. [PubMed: 19336841]
18. Adams ML, Larsen EW. Fast iterative methods for discrete ordinates particle transport calculations. *Prog Nucl Energy*. 2002; 40(1):3–159.
19. Montejo LD, Klose AD, Hielscher AH. Implementation of the equation of radiative transfer on block-structured grids for modeling light propagation in tissue. *Biomed Opt Express*. 2010; 1:861–878. [PubMed: 21258514]
20. Ren K, Abdoulaev GS, Bal G, Hielscher AH. Algorithm for solving the equation of radiative transfer in the frequency domain. *Opt Lett*. Mar.2004 29:578–580. [PubMed: 15035476]
21. Fletcher JK. A solution of the neutron transport equation using spherical harmonics. *J Phys A: Math Gen*. 1983; 16:2827–2835.
22. Kobayashi K, Oigawa H, Yamagata H. The spherical harmonics method for the multigroup transport equation in x-y geometry. *Ann Nucl Energy*. 1986; 13(12):663–678.
23. Jha AK, Kupinski MA, Masumura T, Clarkson E, Maslov AA, Barrett HH. Simulating photon-transport in uniform media using the radiative transport equation: A study using the Neumann-series approach. *J Opt Soc Amer A*. 2012; 29(8):1741–1757.
24. Jha AK, Kupinski MA, Barrett HH, Clarkson E, Hartman JH. A three-dimensional Neumann-series approach to model light transport in non-uniform media. 2012
25. Lehtikangas O, Tarvainen T, Kim A, Arridge S. Finite element approximation of the radiative transport equation in a medium with piece-wise constant refractive index. *Journal of Computational Physics*. 2015; 282:345–359.
26. Haskell RC, Svaasand LO, Tsay TT, Feng TC, McAdams MS, Tromberg BJ. Boundary conditions for the diffusion equation in radiative transfer. *J Opt Soc Am A Opt Image Sci Vis*. Oct.1994 11:2727–2741. [PubMed: 7931757]

27. Jha, AK., Zhu, Y., Dreyer, J., Kang, J., Gjedde, A., Wong, D., Rahmim, A. [Biomedical Optics 2016], Biomedical Optics 2016. Optical Society of America; 2016. Incorporating boundary conditions in the integral form of the radiative transfer equation for transcranial imaging. JW3A.47
28. Jha AK. Retrieving information from scattered photons in medical imaging. 2013
29. Schweiger M, Arridge SR, Hiraoka M, Delpy DT. The finite element method for the propagation of light in scattering media: boundary and source conditions. Med Phys. Nov.1995 22:1779–1792. [PubMed: 8587533]
30. Jha AK, Clarkson E, Kupinski MA. An ideal-observer framework to investigate signal detectability in diffuse optical imaging. Biomed Opt Express. 2013; 4(10):2107–2123. [PubMed: 24156068]

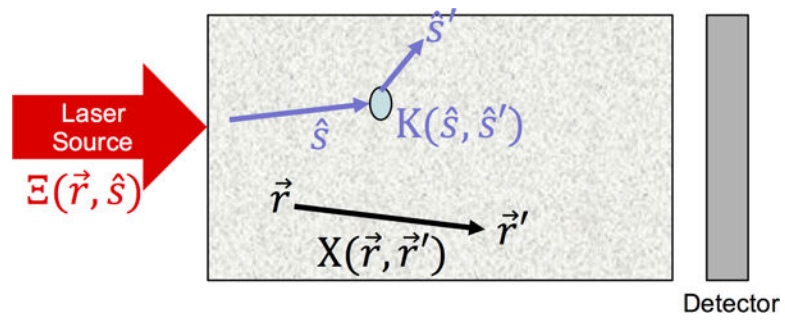


Figure 1.
The various mathematical operators used to describe the Neumann-series RTE

$$w = X\Xi + XKX\Xi + XKXKX\Xi + \dots$$

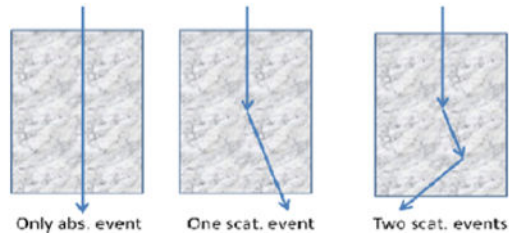


Figure 2. A schematic illustrating the physical interpretation of the different terms in the Neumann series RTE²³

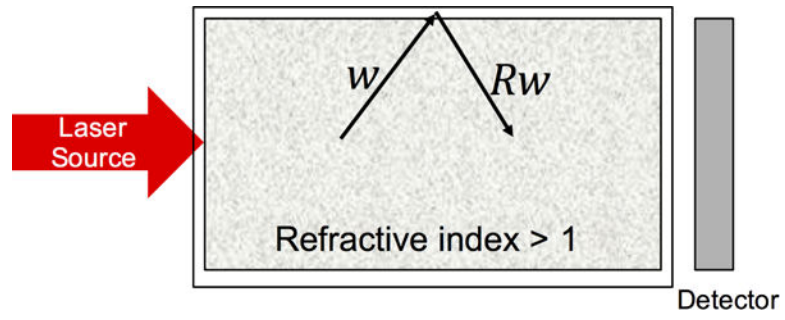


Figure 3. Schematic illustrating the thin boundary and the effect of reflection operator.

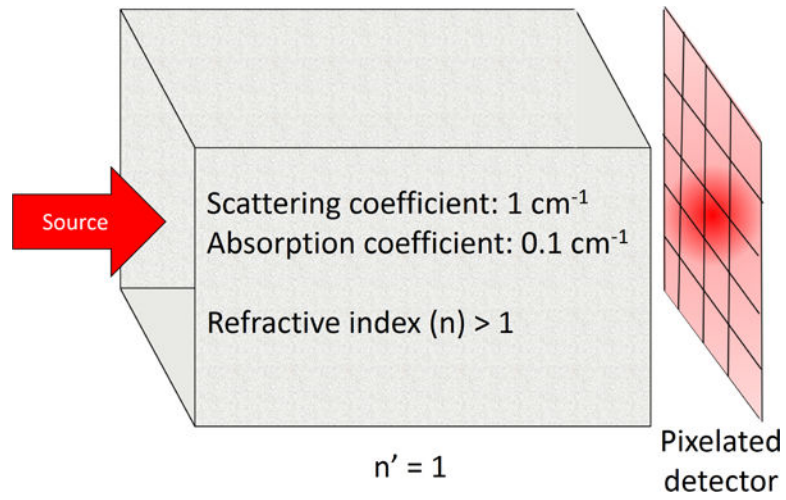


Figure 4.
The experimental setup simulated to evaluate the proposed framework

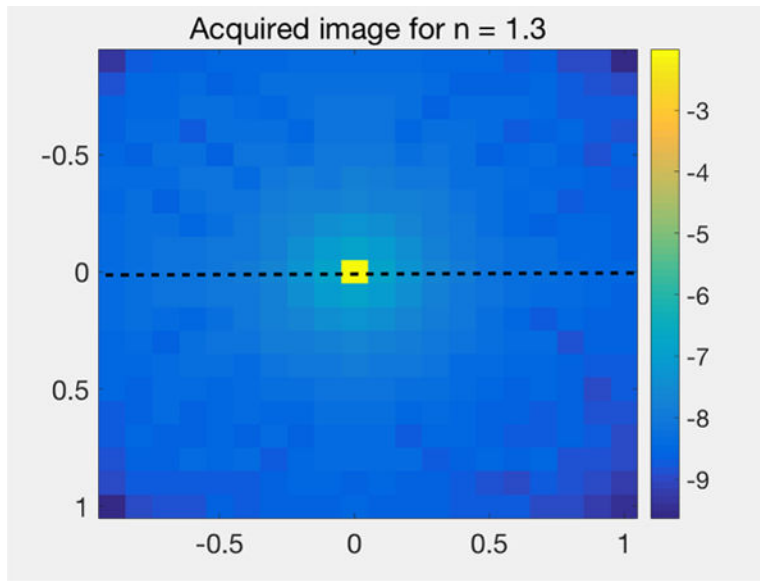


Figure 5. Representative output image with the proposed method when refractive index of the medium was 1.3

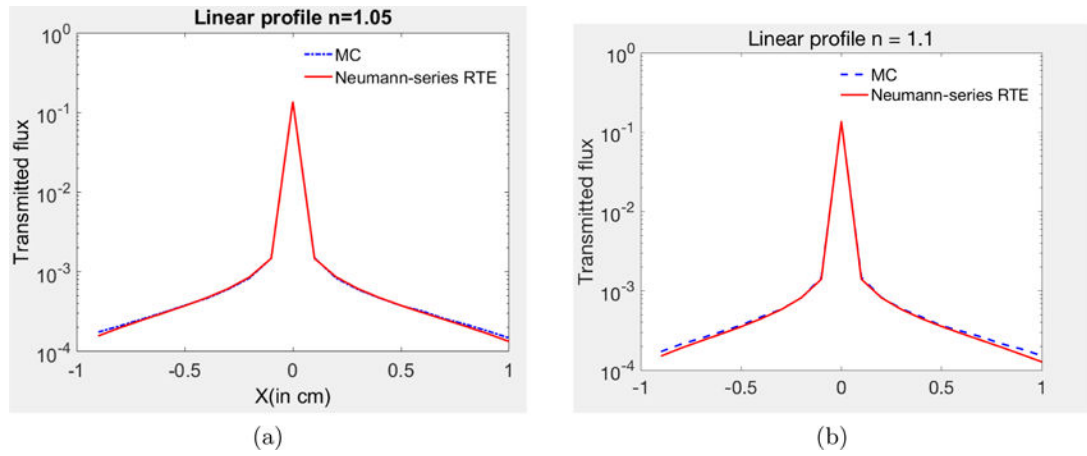


Figure 6. Comparison of the linear profiles of the images obtained with the MC and proposed Neumann-series RTE formalisms, when the refractive index of the scattering medium is (a) 1.05 (b) 1.1

Table 1

Error between MC output and Neumann-series output with and without boundary conditions

Refractive index n	RTE without boundary conditions	RTE with boundary conditions
1.05	1.25%	0.85%
1.1	3.23%	1.48%

Author Manuscript

Author Manuscript

Author Manuscript

Author Manuscript